A COMPARATIVE ASSESSMENT OF LAND USE-LAND COVER DYNAMICS BETWEEN BANGLADESH AND INDIAN SUNDARBANS FROM 1975-2020: A GEOSPATIAL AND STATISTICAL-BASED APPROACH

A.H. Kanan[1]*, F. Pirotti[1,2]

[1]Department of Land, Environment, Agriculture and Forestry (TESAF), University of Padova. Via dell'Università 16, 35020 Legnaro (PD), Italy - kanan.sust@gmail.com

[2]Interdepartmental Research Center of Geomatics (CIRGEO), University of Padova. Via dell'Università 16, 35020 Legnaro (PD), Italy - francesco.pirotti@unipd.it

Commission III, WG III/7

KEY WORDS: Sundarbans mangrove, Landsat, LULC, Accuracy assessment, Anthropogenic disturbances, Climate change, Bangladesh, India.

ABSTRACT:

The study aims to compare land use land cover (LULC) change between Bangladesh and Indian Sundarbans from 1975 to 2020 using Landsat Satellite images. We performed supervised maximum likelihood (ML) to classify the study area at four time periods over 45 years (1975, 1990, 2005, and 2020). The classification was assigned to five classes: dense forest, moderate forest, sparse forest, barren land, and water body. Accuracy assessment of the classified images was completed with 250 control points for each year. The findings of our study revealed that the dense forest cover of Bangladesh and Indian parts was 54% and 31%, respectively, whereas, for the whole Sundarbans, it was 45% in 1975. However, the dense forest of Bangladesh and Indian Sundarbans decreased by an annual rate of 1.20% and 1.60%, respectively, from 1975 to 2020. From 1990 to 2005, Bangladesh Sundarbans slightly increased the dense forest cover by an annual rate of 0.68%, while the Indian Sundarbans decreased by an annual rate of 0.63%. The moderate dense forest of Bangladesh and Indian Sundarbans increased by giving almost the same annual rate of 3.62% and 3.59% from 1975 to 2020, whereas the increasing rate of the sparse forest was much higher for Bangladesh (8.36%) Sundarbans than Indian (3.36%) parts. The water bodies of Bangladesh and Indian Sundarbans increased by giving an annual rate of 0.48% and 0.71%, respectively, from 1975 to 2020. Our study found that most of the barren lands were located near the boundary between forest and human settlement of Indian Sundarbans compared to Bangladesh. The findings of the comparative assessment between these two countries can support sustainable forest management and planning by considering the best policy options.

1. INTRODUCTION

Mangroves are salt-tolerant trees and shrubs (Awty-Carroll et al., 2019; Long and Giri, 2011), forming forests in the intertidal zone between sea and land (Islam et al., 2019; Datta and Deb, 2012). The spatial distribution of the mangrove forests is in the tropical and subtropical regions of the world (FAO, 2010). The most significant extent of mangroves is found in South and Southeast Asia (41%), with the rest distributed across various regions (59%) (Malik et al., 2017; Giri et al., 2011). Sundarbans is the world's largest contiguous mangrove forest, accounting for 3% of the global mangrove forest area (Chanda et al., 2016). It spans 10,000 km^2, with 62 % (6,200 km^2) in Bangladesh and the remaining 38% (3800 km^2) in India (Ghosh et al., 2015).

Sundarbans offer numerous ecosystem goods and services to coastal populations (Payo et al., 2016; FAO, 2010). Approximately 3.5 million Bangladeshis and 4 million Indians are dependent on these ecosystem goods and services. Sundarbans act as a natural barrier to protect storms, cyclones, tsunamis and coastal soil erosion for coastal settlements (Hasan et al., 2020; Islam et al., 2019). In addition, Sundarbans is considered a biological supermarket and hotspot for biodiversity conservation (Payo et al., 2016). For instance, Sundarbans provide a habitat for many threatened and endangered species like the Royal Bengal tiger (Ortolano et al., 2016).

The ecological and socioeconomic aspects of the Sundarbans are a single unit (Ortolano et al., 2016). But, the Sundarbans are managed separately by Bangladesh and India, prioritizing their management policies after the partition of India in 1947. For instance, to protect Sundarbans and its wildlife, Bangladesh Sundarbans were divided into three wildlife sanctuaries (1977): Sundarbans east, west, and south. Latter, Ecologically Critical Area (ECA) and Sundarbans Impact Zone (SIZ) were declared to protect the forest from human disturbances (Nishat et al., 2019). However, the areas and density of Bangladesh and Indian Sundarbans are decreasing significantly due to both human-induced – e.g., over exploitation of resources, agricultural expansion, industrialization, etc. – and natural factors -e.g., cyclonic storms, sea level and salinity rise, and so on (Quader et al., 2017; Loucks, et al., 2010; Islam, 2010; Gopal and Chauhan, 2006). According to Das and Datta (2016), anthropogenic activities are one of the key drivers of Sundarbans ecological degradation. In addition, the Sundarbans ecosystems are highly susceptible to climate change-related

* Corresponding author

hazards. For instance, the sea-level in Sundarbans regions is much higher (+3.90±0.46 mm/year) (Nishat et al., 2019) than the global rate (1.0–2.0 mm/year) (Deb and Ferreira, 2017; Karim and Mimura, 2008). Giri et al. (2007) reported that the Sundarbans mangrove forest area decreased by 1.2% from 1970 to 2000 due to anthropogenic activities and climate change-related factors. Therefore, the Sundarbans are one of the most vulnerable tropical ecosystems on the planet.

Most of the areas of Sundarbans are inaccessible due to forest geophysical features and other adverse environmental conditions (Datta and Deb, 2012; Emch and Peterson, 2006). Moreover, the legal borderline between Bangladesh and India makes it difficult to present an overview about the evolution and current state of the whole Sundarbans (Ishtiaque and Chhetri, 2016; Giri et al., 2014; Gopal and Chauhan, 2006). In this situations the application of remote sensing is useful for detecting and monitoring Sundarbans LULC changes overtime (Quader et al., 2017). However, the study on entire Sundarbans is scanty (Hasan et al., 2020; Islam et al., 2019), and most studies have been done separately in Bangladesh or Indian Sundarbans. Furthermore, different time frames, seasons, sensors, classifications techniques have been used independently for mapping LULC of Bangladesh and Indian Sundarbans, which is not comparable to tracking and discussing the numerous causes of LULC change between two countries. For example, Quader et al. (2017) studied LULC of entire Sundarbans by highlighting some limitations and absence of comparison between Bangladesh and Indian Sundarbans. In the case of Sundarbans (a single forest unit separately managed by Bangladesh and India), the comparative assessment of LULC is important to recognize the effectiveness of forest management policies are applied independently by these countries against human impacts and climatic change hazards. Giri et al. (2007) classified the entire Sundarbans with mangrove and non-mangrove categories. However, the detailed classification of mangrove vegetations (e.g., dense, moderate dense, and sparse forest) is essential to understand the forest structure and density, which Bangladesh and India follow for forest management perspective. Our study tries to overcome these limitations to find out the LULC changes of Sundarbans over time.

The study aims to find and comparative assessment LULC classes (e.g., dense, moderate dense, sparse forest, barren land, and water body) of Bangladesh and Indian Sundarbans using Landsat data from 1975 to 2020.

2. METHODOLOGY

2.1 Description of the study area

The present study considered the entire Sundarbans areas (covering Bangladesh and Indian part), which lies between 21°32′ and 22°40′ N and 88°05′ and 89°51′ E. (Figure 1). The Sundarbans are formed on the estuary created by the Hooghly, Ganges, Brahmaputra, and Meghna rivers in the Bay of Bengal (Deb and Ferreira, 2017). These rivers are the key source of freshwater and sediment to Sundarbans. The elevation of forest floor ranges from 1.5 to 3 m mean sea level, and it is interlinked by a complex network of tidal rivers, mudflats, and small islands (Karim and Mimura, 2008). The forest is inundated twice daily by the tide (Barlow et al., 2011). The climate is tropical, with a dry season from December to February and a monsoonal rainy season from March to November (Quader et al., 2017). The tropical cyclones and storms hit Sundarbans regularly during the monsoon, causing severe flooding and wind damage (Ghosh et al., 2015).

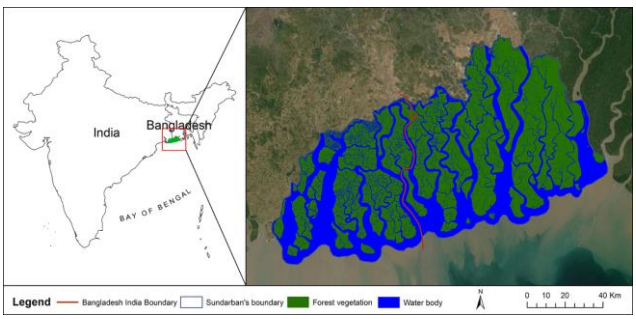

Figure 1. Sundarbans mangrove forest, including Bangladesh and Indian parts. The red line on the map indicates the international boundary between the two countries.

Year	Date and time of image acquisition	Used satellite/sensor	Path/Row	Used brand	Spatial resolution	Cloud cover	Sun angle	Covered area*
1975	Feb 19, 1975 / 9:45 am	L 2 / MSS	147 / 045	4-7	60 m	0%	40.86	BS
	Jan 10, 1976 / 9:47 am	L 2 / MSS	148 / 045	4-7	60 m	0%	33.95	IS, BS
	Jan 10, 1976 / 9:48 am	L 2 / MSS	148 / 044	4-7	60 m	0%	33.02	BS
1990	Feb 24, 1990 / 9:46 am	L 5 / TM	137 / 045	1-7	30 m	0%	42.26	BS
	Jan 14, 1990 / 9:54 am	L 5 / TM	138 / 045	1-7	30 m	0%	34.86	IS, BS
2005	Jan 16, 2005 / 10:11 am	L 5 / TM	137 / 045	1-8	30 m	0%	38.55	BS
	Jan 07, 2005 / 10:17 am	L 5 / TM	138 / 045	1-8	30 m	0%	37.82	IS, BS
2020	Jan 26, 2020 / 10:25 am	L 8 / OLI-TIRS	137 / 045	1-7	30 m	0%	41.79	BS
	Jan 17, 2020 / 10:32 am	L 8 / OLI-TIRS	138 / 045	1-7	30 m	0.62%	40.46	IS, BS

Table 1. Source and specification of satellite images used in the study. Covered area*: BS=Bangladesh Sundarbans, IS=Indian Sundarbans

2.2 Image selection

We collected nine Level-1 Terrain (L1T) Landsat scenes from the United States Geological Survey (USGS). These scenes were used for quantifying LULC change for four-time periods (1975, 1990, 2005, and 2020) (Table 1). With the exception of 1975, the radiometrically and geometrically calibrated Landsat

scenes were retrieved from Earth Explorer (https://earthexplorer.usgs.gov/). Except for one scene (2020), the other cloud-free scenes were collected between January to February, which fells in the cold-dry season (November-March). The mangroves are evergreen forests, and leaves have a longer lifespan; leaves are not off during the leaf-fall season (December to February) in the study area. Therefore, there is no significant variation in vegetation phenology and spectral signature between January and February (Islam et al., 2019; Bera and Chatterjee, 2019). The mangrove forest floor is inundated twice a day by the tide, and LULC mapping using satellite data is influenced by the tidal range (e.g., high, low, and mid-tide) (Zhang et al., 2015). However, Landsat satellites fly and capture the images of Sundarbans regions when it is in mid-tide level; and is the best condition for LULC mapping of Sundarbans mangroves.

Landsat Multi-Spectral Scanner (MSS) for 1975, Thematic Mapper (TM) for 1990 and 2005, and Operational Land Imager-Thermal Infrared Sensor (OLI-TIRS) for 2020 were used to classify LULC of Sundarbans. In the case of 1975, three adjacent Landsat-2 (MSS) scenes are needed to cover the entire Sundarbans. The source and other specifications of the used satellite images (e.g., brand, spatial resolution, and so on) of Sundarbans are given in Table 1.

2.3 Image pre-processing

The satellite image pre-processing is a crucial part that includes radiometric calibration, atmospheric correction, cloud masking, image mosaicking, study area extraction, and image rectification (Banskot et al., 2014; Gao et al., 2009). Except for Landsat-2 (MSS) images of 1975, the others were radiometrically and geometrically calibrated and thoroughly been used for subsequent analyses (Sannigrahi et al., 2019). In this study, the Landsat-2 (MSS) images were processed by standard procedures such as image calibration to at-sensor radiance, then radiometric correction was completed using an atmospheric correction model to get surface reflectance images. These correction steps were applied to the images using the Fast Line-of-sight Atmospheric Analysis of Spectral Hypercubes (FLAASH) tools based on a MODTRAN radiative transfer module of ENVI 5.3 software (Hasan et al., 2020). FLAASH is a well-known and advanced atmospheric correction algorithm used in remote sensing platforms (Serrano et al., 2016), and it produces more accurate results than other methods (Smith, 2015). The FLAASH model includes a method for reducing the inconsistency of radiometric and atmospheric (i.e., water vapor, haze, smoke, fog, dust, aerosol) effect in images (Matthew et al., 2020; Kaufman et al., 1997).

We performed cloud masking only for one Landsat-8 (OLI-TIRS) images (MSS and TM images were cloud free). To mosaic each epoch Landsat image, seamless mosaicking was used. We also applied the modified pseudo-invariant features (PIF) method as part of the relative radiometric correction of the scenes of the Landsat sensor (Myeong et al., 2006). The PIF approach eliminates inconsistencies across scenes in the same mosaic of images (Quader et al., 2017). After mosaicking, the study area was extracted by considering the administrative boundary of Sundarbans, and then images were composited with near-infrared, red, and green bands for classification.

We used 50 ground control points for image rectification, and the dispersed ground control points were generated using a root mean square error (RMSE). The lower RMSE stands higher the accuracy of LULC prediction (Talukdar et al., 2020). In this study, the maximum RMSE was 0.39, belonging to the acceptable range for LULC change detection (Knorn et al., 2009; Tucker et al., 2004). After that, the images were resampled to a 30 m pixel size using the nearest neighbour resampling method (Ghosh et al., 2017).

2.4 Training sample selection, image classification and accuracy assessment

The training samples were selected manually by careful inquiry of homogenous pixels of LULC classes (e.g., dense, moderate dense, sparse forest, barren land, and water body). High-resolution Google Earth images were used as a reference to identify the actual LULC classes. However, a sufficient number of training samples are prerequisites for a successful and superior classification (Lu and Weng, 2007). Moreover, the tidal range (e.g., high, low, and mid-tide) and upstream flow influences mangrove LULC mapping using satellite data (Zhang et al., 2015). For instance, the watercolor is different near the coastal/beach/shoreline areas than the deep river basins of Sundarbans due to the sedimentation, water deepness, and tidal effect; thus, the spectral variation is a little different. In this case, we considered numerous water body sites for training samples. Finally, 245 training samples throughout the area for each study year were selected to identify the LULC classes (a total of 980 training samples for four study years: 1975, 1990, 2005, and 2020). The training samples were distributed among the LULC classes as follows: 50 samples for dense forest, 50 for moderate dense forest, 45 for sparse forest, 35 for barren land, and 65 for water bodies.

A variety of image classification techniques are used for mapping and studying LULC change (Billah et al., 2021; Lu and Weng, 2007). Supervised classification using maximum likelihood (ML) algorithm have been used worldwide over the past two decades to study mangrove LULC (Kumar et al., 2021; Islam et al., 2019; Bera and Chatterjee, 2019; Jones et al., 2016; Ghosh et al., 2016; Pham and Yoshino, 2015; Chen et al., 2013; Giri et al., 2010; Giri and Muhlhausen 2008; Giri et al. 2007). Because, the ML algorithm is one of the most well-known parametric classifiers used for supervised classification (Li et al., 2014) and is easy to use, thus, an extended training process is not essential (Chen et al., 2013; Datta and Deb, 2012). Moreover, the ML algorithm reduces the data necessities and delivers a prospective to extract comprehensive information (Hassan, 2017; Jat et al., 2017) by computing the weighted distance or likelihood of an unknown measurement vector that belongs to one of the known classes, based on the Bayesian equation. The unknown measurement vector is assigned to the class based on the highest probability of fit. Furthermore, consideration of a variance-covariance matrix within the class distributions is considered one of the advantages of this algorithm. In addition, consideration of a variance-covariance matrix within the class distributions is another advantage of this algorithm (Ghosh et al., 2016). In this study, we performed supervised maximum likelihood (ML) to classify the study area at four time periods over 45 years (1975, 1990, 2005, and 2020). The classification was assigned to five classes: dense forest, moderate forest, sparse forest, barren land, and water body.

Validation of classified images is vital to study LULC change over time (Ghosh et al. 2016; Sinha et al. 2014). In this study, we randomly selected 250 control points for each study year

over the classified images to measure accuracy (a total of 1000 control points for four study years). The points were labeled based on land cover within a 30 m radius; if a point fell too close to two different land cover classes, it was slightly adjusted to ensure that it was representative of a full Landsat pixel. Google Earth historical images were used to verify these check-points. However, there is no information in Google Earth's historical images for 1975. In this case, we verified the images through previous literature, expert-based information (Quader et al., 2017), and historical toposheet maps (sheet NF 45-8, series U 502) from the survey of India. Classification accuracy for the classified images was assessed by computing error metrics (producer, user, and overall accuracy) and kappa coefficients (K) (Kanniah et al., 2015; Stehman, 1996). The value of K equal to one indicates perfect agreement, whereas a value close to zero indicates agreement that is no better than would be expected by chance. (Rwanga and Ndambuki, 2017). Therefore, the higher value of K indicates the higher the accuracy of LULC expectation.

2.5 Mapping and analysis LULC

After the accuracy assessment, the final map was carried out for Bangladesh and Indian Sundarbans for four different study years (1975, 1990, 2005, and 2020). Then, we calculated periodic LULC change from one year to another. The calculation corresponds to equations (1) and (2). Finally, the causes of periodic change patterns were discussed in terms of human-induced (i.e., agricultural, industrial activities, and encroachment) and climate change-related factors (i.e., sea level and salinity rise, cyclonic storms, and soil erosions):

$$LULC_{(t)} = LULC_{(t_2)} - LULC_{(t_1)} \quad (1)$$

$$LULC_{(t_r)} = \frac{LULC_{(t_2)} - LULC_{(t_1)}}{LULC_{(t_1)}} \times \frac{1}{t} \times 100 \quad (2)$$

where $LULC_{(t)}$ = LULC change between two periods
t_1 = starting period
t_2 = ending period
$LULC_{(t_r)}$ = LULC rate between two periods
t = total number of years between two periods

3. RESULTS

The geospatial maps exposed that the dense forest was Sundarbans' dominant land cover type in 1975. Most of the dense forest areas are located in the Bangladesh part of Sundarbans compared to Indian ones from 1975 to 2020. On the other hand, the sparse forest and barren land areas were highest in the Indian part of Sundarbans than in Bangladesh. However, the maximum barren land areas are located near to borderline between forest and human habitat (Figure 2).

The findings of our study revealed that the dense forest cover of Bangladesh and Indian parts was 54% and 31%, respectively, whereas, for the whole Sundarbans, it was 45% in 1975. However, the Indian Sundarbans decreased dense forest cover continuously from 1975 to 2020. Similarly, the Bangladesh Sundarbans decreased dense forest, except in 2005. In 1975, the second main class cover for Bangladesh Sundarbans was water, followed by moderate dense, barren land and sparse forest.

LULC	Area (ha) (% of total area)											
	1975			1990			2005			2020		
	BS	IS	WS	BS	IS	WS	BS	IS	WS	BS	IS	WS
Dense forest	335444 (54)	117253 (31)	452697 (45)	209144 (33)	56533 (15)	265677 (27)	230596 (37)	51208 (14)	281805 (28)	153087 (25)	33279 (9)	186366 (19)
Moderate - dense forest	55300 (9)	25509 (7)	80810 (8)	146403 (23)	35312 (10)	181715 (18)	118601 (19)	54809 (15)	173411 (17)	145391 (23)	66641 (18)	212032 (21)
Sparse forest	21492 (3)	31516 (9)	53007 (5)	63878 (10)	109628 (29)	173506 (17)	61287 (10)	75019 (20)	136306 (14)	102298 (16)	79231 (21)	181530 (18)
Barren land	35922 (6)	64091 (17)	100013 (10)	11677 (2)	29899 (8)	41576 (4)	20472 (3)	31693 (8)	52164 (5)	8883 (1)	15780 (4)	24664 (2)
Water bodies	178699 (28)	135336 (36)	314035 (32)	196866 (32)	143862 (38)	340728 (34)	197045 (31)	162495 (43)	359540 (36)	217311 (35)	178859 (48)	396170 (40)

Table 2. LULC of Sundarbans from 1975 - 2020. Here, BS=Bangladesh Sundarbans, IS=Indian Sundarbans, WS=Whole Sundarbans

However, the second main class cover for Indian Sundarbans was dense forest, followed by barren land, sparse forest, and moderate dense forest (Table 2). The sequence of different land cover classes for both countries was changed by increasing and decreasing the engaged areas from 1975 to 2020. Consequently, in 2020, most of the dense forest of Bangladesh and Indian Sundarbans was reduced by water and moderate dense forest. As a result, the water body covered maximum areas for both countries, and the dense forest cover of Bangladesh (25%) and Indian (9%) Sundarbans placed with the second and fourth position in 2020 (Table 2).

The dense forest of Bangladesh and Indian Sundarbans decreased by an annual rate of 1.20% and 1.60%, respectively, from 1975 to 2020. However, the annual decreasing rate for the whole Sundarbans was 1.30%. From 1990 to 2005, Bangladesh Sundarbans slightly increased the dense forest cover class by an annual rate of 0.68%, while the Indian Sundarbans decreased by an annual rate of 0.63%. The moderate dense forest of Bangladesh and Indian Sundarbans increased by giving almost the same annual rate of 3.62% and 3.59% from 1975 to 2020, whereas the increasing rate of the sparse forest was higher for Bangladesh (8.36%) Sundarbans than Indian (3.36%) parts. The water bodies of Bangladesh and Indian Sundarbans increased by giving an annual rate of 0.48% and 0.71%, respectively, from 1975 to 2020.

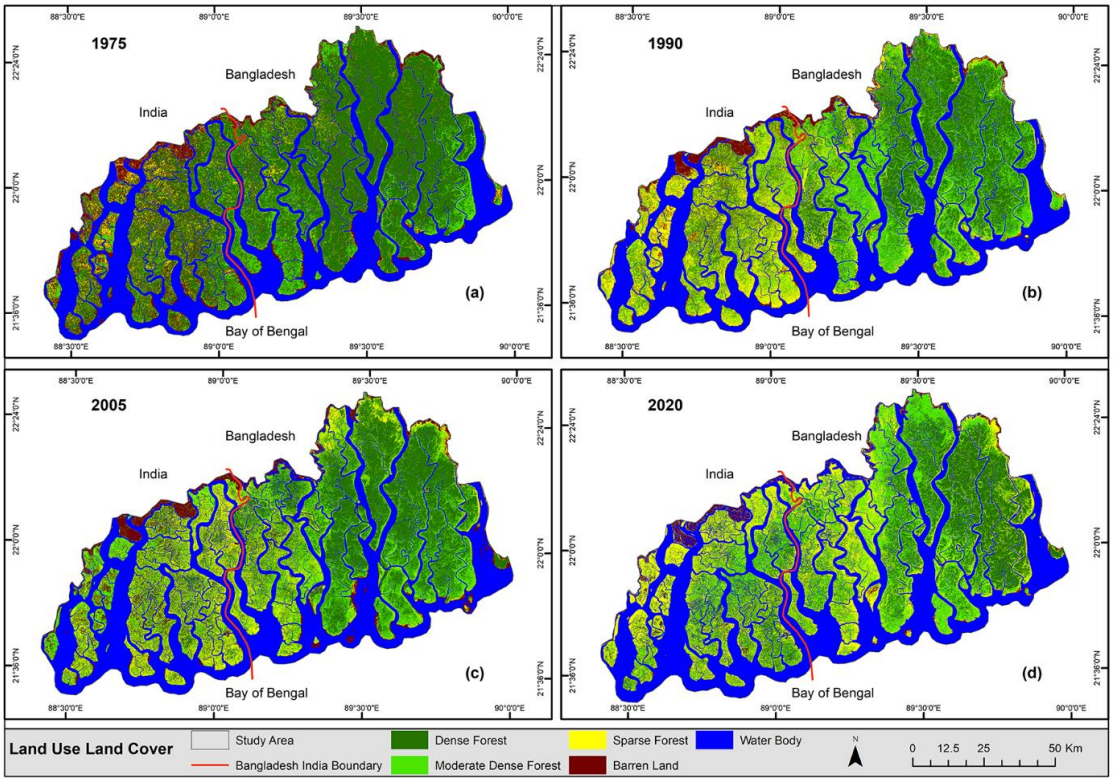

Figure 2. LULC of Bangladesh and Indian Sundarbans from 1975 to 2020 (red line is the boundary between Bangladesh and India)

4. DISCUSSION

Environmental disturbances that drive changes in forest cover can be monitored efficiently by remote sensing means (Piragnolo et al., 2021; Vaglio Laurin et al., 2016). Anthropic interaction is a key factor globally (Mozzato et al., 2018; Pagliacci et al., 2020). Active remote sensing technologies like radar and lidar can extract detailed biomass maps (LaRocque et al., 2020; Pirotti et al., 2014), but are more expensive .

The dense and moderate forest cover was higher in the Bangladesh Sundarbans compared to the Indian part (1975-2020). Moreover, the annual decreasing rate of the dense forest was higher in Indian Sundarbans (1.60%) than in Bangladesh (1.20%). The reason might account mainly for the intensity of soil and water salinity of the Sundarbans. Gopal and Chauhan (2006) reported that the salinity decreases from west to east of Sundarbans and dominates by less salinity lovers *Heritiera*

LULC	Area changes (ha) (Annual rate of changes %)											
	1975-1990			1990-2005			2005-2020			1975-2020		
	BS	IS	WS	BS	IS	WS	BS	IS	WS	BS	IS	WS
Dense forest	-126300 (-2.51)	-60720 (-3.45)	-187020 (-2.75)	+21452 (+0.68)	-5325 (-0.63)	+16128 (+0.40)	-77509 (-2.24)	-17929 (-2.33)	-95439 (-2.25)	-182357 (-1.20)	-83974 (-1.60)	-266331 (-1.30)
Moderate - dense forest	+91103 (+10.98)	+9803 (+2.56)	+100905 (+8.31)	-27802 (-1.27)	+19497 (+3.68)	-8304 (-0.30)	+26790 (+1.50)	+11832 (+1.44)	+38621 (+1.48)	+90091 (+3.62)	+41132 (+3.59)	+131222 (+3.61)
Sparse forest	+42386 (+13.14)	+78112 (+16.52)	+120499 (+15.15)	-2591 (-0.27)	-34609 (-2.10)	-37200 (-1.43)	+41011 (+4.46)	+4212 (+0.37)	+45224 (+2.21)	+80806 (+8.36)	+47715 (+3.36)	+128523 (+5.39)
Barren land	-24245 (+4.50)	-34192 (+3.55)	-58437 (+3.90)	+8795 (+5.02)	+1794 (+0.40)	+10588 (+1.70)	-11589 (-3.77)	-15913 (-3.35)	-27500 (-3.51)	-27039 (-1.67)	-48311 (-1.68)	-75349 (-1.67)
Water bodies	+18167 (+0.68)	+8526 (+0.42)	+26693 (+0.57)	+179 (+0.01)	+18633 (+0.86)	+18812 (+0.37)	+20266 (+0.69)	+16364 (+0.67)	+36630 (+0.68)	+38612 (+0.48)	+43523 (+0.71)	+82135 (+0.58)

Table 3. Analysis LULC changes of Sundarbans from 1975 - 2020. The analysis was based on estimating net and annual rate changes between two periods.

fomes tree (Aziz and Paul, 2015). However, the *Heritiera fomes* dominated forest stands (Bangladesh part) are also decreasing due to increasing soil salinity. Mukhopadhyay et al. (2015) and Aziz and Paul (2015) reported that about 32% of Bangladesh Sundarbans were covered by only *Heritiera fomes* in 1959, which reduced to 21% in 1983 and 17% in 2015. Human-induced activities like dam construction across the river reduce upstream freshwater flow to Sundarbans and increase salinity. For instance, the Ganges waterway decreased freshwater discharge from 3700 m^3s^{-1} in 1962 to 364 m^3s^{-1} in 2006 due to the construction of the Farakka Barrage in 1975, resulting in increasing salinity level of the Bangladesh and Indian Sundarbans and decreasing forest cover (Islam and Gnauck, 2008).The sparse forest and barren land areas were highest in the Indian part of Sundarbans than in Bangladesh. The reasons are that the south-western part of the Indian Sundarbans is degraded mainly for extensive extraction of mangrove resources, fishery development, siltation, cyclonic storm effects, and land erosion (Paul et al., 2017). The study also found that most of the barren lands were near the border between forest and human settlements, indicating human-induced degradation. According to Kumar et al. (2021), settlement and agricultural expansion have reduced the forest-covered area adjacent to Sundarbans' boundary. Neogi et al. (2017) reported that agricultural activities had destroyed around 24,730 ha of Sundarbans mangroves from1975-2010, whereas only shrimp cultivation destroyed 7,550 ha. Sundarbans is an innocent victim of climate change-related hazards. The study showed that the water areas increased in both Bangladesh and Indian Sundarbans from 1975 to 2020. The reason might for the increase in sea level rise and soil erosion. According to Quader et al. (2017), the water bodies and sea levels increased gradually from 1977 to 2010, indicating sea levels reduced in some areas of Sundarbans. Nishat et al. (2019) reported that the sea level rise in the Sundarbans is +3.90±0.46 mm/year, and Ghosh et al. (2015) stated it is 3.14 mm/year. Therefore, sea-level rise increases both surface water and soil salinity (Bhuyian and Dushmanta, 2011) and reduces the forest's diversity and density. The tropical cyclones caused massive damage to the Sundarbans from 1975 to 2020. Most of the cyclonic storms were started landfall in the Indian part of Sundarbans. Therefore, most of the time, the intensity of damage was higher in Indian Sundarbans. According to Samanta et al. (2021), the cyclone Bulbul (2019) damaged 14.6% (303.6 km^2) and 45.8% (950.7 km^2) of Indian Sundarbans areas with high and low loss, respectively.

5. CONCLUSION

The percentages of dense and moderate dense forest were highest in Bangladesh Sundarbans compared to Indian ones. However, both countries decreased dense forest cover by altering it into moderate and sparse areas from 1975 to 2020. The decreasing rate of dense forest was higher for Indian Sundarbans. The sparse forest and barren land areas were highest in the Indian part of Sundarbans than in Bangladesh, and most of the barren lands were near the border between forest and human settlements. Because the areas accessible to human activities are significantly more affected by land cover changes. Along with anthropogenic activities, climate change-related hazards are threats to the degradation of Sundarbans. The findings of this study can help for strategic planning to control human disturbances and environmental aspects (e.g., sea level and salinity rise, cyclonic storms, and soil erosions) to the achievement of some of the United Nations Sustainable Development Goals (UN-SDGs).

REFERENCES

Awty-Carroll, K., Bunting, P., Hardy, A., Bell, G., 2019. Using Continuous Change Detection and Classification of Landsat Data to Investigate Long-Term Mangrove Dynamics in the Sundarbans Region. Remote Sens. 11, 2833. https://doi:10.3390/rs11232833

Aziz, A., Paul, A. R., 2015. Bangladesh Sundarbans: Present status of the Environment and Biota. Diversity 7, 242-269. https://doi:10.3390/d7030242

Banskot, A., Kayastha, N., Falkowski, M. J., Wulder, M. A., Froese, R. E., White, J. C., 2014. Forest monitoring using Landsat time series data: a review. Can J Remote Sens 40(5), 362–384.

Barlow, A. C. D., Smith, J. L. D., Ahmad, I. U., Hossain, A. N. M., Rahman, M., Howlader. A. 2011. Female tiger Panthera tigris home range size in the Bangladesh Sundarbans: The value of this mangrove ecosystem for the species-conservation. Oryx, 45(1), 125-128. https://doi.org/10.1017/S0030605310001456

Bera, S., Chatterjee, N. D., 2019. Mapping and monitoring of land use dynamics with their change hotspot in North 24 Parganas district, India: a geospatial and statistical based approach. Modeling Earth Systems and Environment 5, 1529-1551. https://doi.org/10.1007/s40808-019-00601-2

Bhuyian, M. J. A. N., Dushmanta, D., 2011. Assessing impacts of sea level rise on river salinity in the Gorai river network, Bangladesh. Estuarine, Coastal and Shelf Science 96, 219-227. https://doi.org/10.1016/j.ecss.2011.11.005

Billah, M. M., Rahman, M. M., Abedin, J., Akter, H., 2021. Land cover change and its impact on human–elephant confict: a case from Fashiakhali forest reserve in Bangladesh. SN Applied Sciences 3, 649. https://doi.org/10.1007/s42452-021-04625-1

Chanda, A., Mukhopadhyay, A., Ghosh, T., Akhand, A., Mondal, P., Ghosh, S., Hazra, S., 2016. Blue Carbon Stock of the Bangladesh Sundarban Mangroves: What could Be the Scenario after a Century? Wetlands, 36(6), 1033–1045. https://doi.org/10.1007/s13157-016-0819-7

Chen, C. F., Son, N. T., Chang, N. B., Chen, C.R., Chang, L.Y., Valdez, M., Aceituno, J. L., 2013. Multi-decadal mangrove forest change detection and prediction in Honduras, Central America, with Landsat imagery and a Markov chain model. Remote Sens 5(12) 6408-6426. https://doi.org/10.3390/rs5126408

Datta, D., Deb, S., 2012. Analysis of coastal land use/land cover changes in the Indian Sundarbans using remotely sensed data. Geo-spatial Information Science 15(4), 241-250. https://doi.org/10.1080/10095020.2012.714104

Deb, M., Ferreira, M., 2017. Potential impacts of the Sunderban mangrove degradation on future coastal flooding in Bangladesh. Journal of Hydro-environment Research 17, 30-46. https://doi.org/10.1016/j.jher.2016.11.005

Emch, M., Peterson, M., 2006. Mangrove Forest Cover Change in the Bangladesh Sundarbans from 1989-2000: A Remote Sensing Approach. Geocarto International 21(1), 5-12.

FAO, 2010. Global forest resources assessment 2010: main report. Food and Agriculture Organization of the United Nations. Forestry Paper.

Gao, F., Masek, J. G., Wolfe, R. E. 2009. Automated

registration and orthorectification package for Landsat and Landsat-like data processing. J Appl Remote Sens 3(1), 033515.

Ghosh, A., Schmidt, S., Fickert, T., Nüsser, M., 2015. The Indian Sundarban Mangrove Forests: History, Utilization, Conservation Strategies and Local Perception. Diversity 149-169. https://doi.org/10.3390/d7020149

Ghosh, M. K., Kumar, L., Roy, C., 2016. Mapping Long-Term Changes in Mangrove Species Composition and Distribution in the Sundarbans. Forests 7(12), 305.

Giri, C., Muhlhausen, J., 2008. Mangrove forest distributions and dynamics in Madagascar (1975-2005). Sensors (Basel) 8(4), 2104-2117. https://doi.org/10.3390/s8042104

Giri, C., Ochieng, E., Tieszen, L. L., Zhu, Z., Singh, A., Loveland, T., Masek, J., Duke, N., 2010. Status and distribution of mangrove forests of the world using earth observation satellite data. Global Ecology and Biogeography 20(1), 154-159. https://doi.org/10.1111/j.1466-8238.2010.00584.x

Giri, Chandra, Pengra, B., Zhu, Z., Singh, A., Tieszen, L. L., 2007. Monitoring mangrove forest dynamics of the Sundarbans in Bangladesh and India using multi-temporal satellite data from 1973 to 2000. Estuarine, Coastal and Shelf Science 73, 91-100. https://doi.org/10.1016/j.ecss.2006.12.019

Giri, S., Anirban, M., Sugata, H., Sandip, M., Deborupa, R., Subhajit, G., Tuhin, G., Debasish, M., 2014. A study on abundance and distribution of mangrove species in Indian Sundarban using remote sensing technique. Journal of Coastal Conservation 18, 359-367.

Gopal, B., Chauhan, M., 2006. Biodiversity and its conservation in the sundarban mangrove ecosystem. Aquatic Sciences 68, 338-354.

Hasan, M. E., Nath, B., Sarker, A. H. M. R., Wang, Z., Zhang, L., Yang, X., Nobi, M. N., Røskaft, E., Chivers, D. J., Suza, M., 2020. Applying Multi-Temporal Landsat Satellite Data and Markov-Cellular Automata to Predict Forest Cover Change and Forest Degradation of Sundarban Reserve Forest, Bangladesh. Forests 11 (9), 1-35. https://doi.org/10.3390/f11091016

Hassan, M. M., 2017. Monitoring land use/land cover change, urban growth dynamics and landscape pattern analysis in five fastest urbanized cities in Bangladesh. Remote Sens Appl Soc Environ 7, 69-83. https://doi.org/10.1016/j.rsase.2017.07.001

Ishtiaque, A., Chhetri, N., 2016. Competing policies to protect mangrove forest: a case from Bangladesh. Environmental Development 19, 75-83.

Islam, M. M., Borgqvist, H., Kumar, L., 2019. Monitoring Mangrove forest landcover changes in the coastline of Bangladesh from 1976 to 2015. Geocarto International, 34(13), 1458-1476. https://doi.org/10.1080/10106049.2018.1489423

Islam, M. M., Borgqvist, H., Kumar, L., 2019. Monitoring Mangrove forest landcover changes in the coastline of Bangladesh from 1976 to 2015. Geocarto International 34(13), 1458-1476. https://doi.org/10.1080/10106049.2018.1489423

Islam, S. N, Gnauck, A., 2008. Mangrove wetland ecosystems in Ganges-Brahmaputra delta in Bangladesh. Frontiers of Earth Science in China 2 (4): 439-448. https://doi.org/10.1007/s11707-008-0049-2

Jat, M. K., Garg, P. K., Khare, D., 2017. Modelling of urban growth using spatial analysis techniques: a case study of Ajmer City (India). Int J Remote Sens 29 (2), 543-567. https://doi.org/10.1080/01431160701280983

Jones, T. G., Glass, L., Gandhi, S., Ravaoarinorotsihoarana, L., Carro, A., Benson, L., Ratsimba, H. R., Giri, C., Randriamanatena, D., Cripps, G., 2016. Madagascar's mangroves: quantifying nation-wide and ecosystem specific dynamics, and detailed contemporary mapping of distinct ecosystems. Remote Sensing 8(2):106. https://doi:10.3390/rs8020106

Kanniah, K. D., Sheikhi, A., Cracknell, A. P., Goh, H. C., Tan, K. P., Ho, C. S., Rasli, F. N., 2015. Satellite images for monitoring mangrove cover changes in a fast-growing economic region in southern Peninsular Malaysia. Remote Sensing 7(11): 14360-14385. https://doi.org/10.3390/rs71114360

Karim, M. F., Mimura, N. 2008. Impacts of climate change and sea-level rise on cyclonic storm surge floods in Bangladesh, Global Environ. Change 18, 490.500. https://doi.org/10.1016/j.gloenvcha.2008.05.002

Kaufman, Y. J., Wald, A. E., Remer, L. A., Gao, B. C., Li, R. R., Flynn, L., 1997. The MODIS 2.1-□m Channel-Correlation with Visible Reflectance for Use in Remote Sensing of Aerosol. IEEE Transactions on Geoscience and Remote Sensing 35, 1286-1298. https://doi:10.1109/36.628795

Knorn, J., Rabe, A., Radeloff, V. C., Kuemmerle, T., Kozak, J., Hostert, P., 2009. Land cover mapping of large areas using chain classification of neighboring Landsat satellite images. Remote Sensing of Environment 113, 957-964. https://doi:10.1016/j.rse.2009.01.010

Kumar, M., Mondal, I., Pham, Q. B., 2021. Monitoring forest landcover changes in the Eastern Sundarban of Bangladesh from 1989 to 2019. Acta Geophysica 561-577.

LaRocque, A., Phiri, C., Leblon, B., Pirotti, F., Connor, K., Hanson, A., 2020. Wetland Mapping with Landsat 8 OLI, Sentinel-1, ALOS-1 PALSAR, and LiDAR Data in Southern New Brunswick, Canada. Remote Sens. 12, 2095. https://doi.org/10.3390/rs12132095

Li, C., Wang, J., Wang, L., Hu, L., Gong, P., 2014. Comparison of classification algorithms and training sample sizes in urban land classification with Landsat thematic mapper imagery. Remote Sens 6, 964-983. https://doi.org/10.3390/rs6020964

Long, G. B., Giri, C., 2011. Mapping the Philippines' Mangrove Forests Using Landsat Imagery. Sensors 11, 2972-2981. https://doi:10.3390/s110302972

Loucks, C., Mayer, S. B., Hossain, M. A. A., Barlow, A., Chowdhury, R. M., 2010. Sea level rise and tigers: predicted impacts to Bangladesh's Sundarbans mangroves: a letter. Climate Change 98, 291-298.

Lu, D., Weng, Q., 2007. A survey of image classification methods and techniques for improving classification performance. Int J Remote Sens 28, 823–870.

Malik, A., Mertz, O., Fensholt, R., 2017. Mangrove forest decline: Consequences for livelihoods and environment in South Sulawesi. Regional Environmental Change 17, 157-169. https://doi.org/10.1007/s10113-016-0989-0

Mandal, D.B., 2007. Man in Biosphere: A Case Study of Sundarban Biosphere Reserve. Gyan Publishing House, New Delhi, India.

Matthew, M. W., Adler-Golden, S. M., Berk, A., Richtsmeier, S. C., Levine, R. Y., Bernstein, L. S., Acharya, P. K., Anderson,

G. P., Felde, G. W., Hoke, M. P., Ratkowski, A., Burke, H. H., Kaiser, R. D., & Miller, D. P., 2000. Status of Atmospheric Correction Using a MODTRAN4-based Algorithm. SPIE Proceedings, Algorithms for Multispectral, Hyperspectral, and Ultraspectral Imagery, 4049, 199-207.

Mozzato, D., Gatto, P., Defrancesco, E., Bortolini, L., Pirotti, F., Pisani, E., Sartori, L., Mozzato, D., Gatto, P., Defrancesco, E., Bortolini, L., Pirotti, F., Pisani, E., Sartori, L., 2018. The Role of Factors Affecting the Adoption of Environmentally Friendly Farming Practices: Can Geographical Context and Time Explain the Differences Emerging from Literature? Sustainability 10, 3101. https://doi.org/10.3390/su10093101

Myeong, S., Nowak, D. J., Duggin, M. J., 2006. A temporal analysis of urban forest carbon storage using remote sensing. Remote Sensing of Environment 101(2), 277-282. https://doi:10.1016/j.rse.2005.12.001

Neogi, S. B., Dey, M., Kabir, S. L., Masum, S. J. H., Kopprio, G., Yamasaki, S., Lara, R., 2017. Sundarban mangroves: diversity, ecosystem services and climate change impacts. Asian Journal of Medical and Biological Research 2(4), 488-507. https://doi.org/10.3329/ajmbr.v2i4.30988

Nishat, B., Rahman, A. J. M. Z., Mahmud, S., 2019. Landscape Narrative of the Sundarban : Towards Collaborative Management by Bangladesh and India, 1-207. http://documents.worldbank.org/curated/en/539771546853079693.

Ortolano, L., Sánchez-Triana, E., Paul, T., Ferdausi, S. A., 2016. Managing the Sundarbans region: Opportunities for mutual gain by India and Bangladesh. International Journal of Environment and Sustainable Development 15(1), 16–31.

Pagliacci, F., Defrancesco, E., Mozzato, D., Bortolini, L., Pezzuolo, A., Pirotti, F., Pisani, E., Gatto, P., 2020. Drivers of farmers' adoption and continuation of climate-smart agricultural practices. A study from northeastern Italy. Sci. Total Environ. 710, 136345. https://doi.org/10.1016/j.scitotenv.2019.136345

Paul, A. K., Ray, R., Kamila, A., Jana, S., 2017. Mangrove degradation in the Sundarbans. In Coastal Wetlands: Alteration and Remediation 21, 357-392. https://doi.org/10.1007/978-3-319-56179-0_11

Payo, A., Mukhopadhyay, A., Hazra, S., Ghosh, T., Ghosh, S., Brown, S., Lázár, A. N., 2016. Projected changes in area of the Sundarban mangrove forest in Bangladesh due to SLR by 2100. Climatic Change 139, 279-291. https://doi.org/10.1007/s10584-016-1769-z

Pham, T. D., Yoshino, K., 2015. Mangrove mapping and change detection using multi-temporal Landsat imagery in Hai Phong city, Vietnam. Paper presented at: The International Symposium on Cartography in Internet and Ubiquitous Environments (Mar 17-19, 2015) Tokyo, Japan.

Piragnolo, M., Pirotti, F., Zanrosso, C., Lingua, E., Grigolato, S., 2021. Responding to Large-Scale Forest Damage in an Alpine Environment with Remote Sensing, Machine Learning, and Web-GIS. Remote Sens. 13, 1541.

Pirotti, F., Laurin, G., Vettore, A., Masiero, A., Valentini, R., 2014. Small Footprint Full-Waveform Metrics Contribution to the Prediction of Biomass in Tropical Forests. Remote Sens. 6, 9576–9599. https://doi.org/10.3390/rs6109576

Quader, M. A, Agrawal, S., Kervyn, M., 2017. Multi-decadal land cover evolution in the Sundarban, the largest mangrove forest in the world. Ocean and Coastal Management 139, 113–124. https://doi.org/10.1016/j.ocecoaman.2017.02.008

Rahman, M. M., Khan, M. N. I., Hoque, A. F., Ahmed, I., 2015. Carbon stock in the Sundarban mangrove forest: spatial variations in vegetation types and salinity zones. Wetlands Ecology and Management, 23, 269-283.

Rwanga, S. S., Ndambuki, J. M., 2017. Accuracy Assessment of Land Use/Land Cover Classification Using Remote Sensing and GIS. International Journal of Geosciences 8, 611-622.

Samanta, S., Hazra, S., Mondal, P. P., Chanda, A., Giri, S., French, J. R., Nicholls, R. J., 2021. Assessment and Attribution of Mangrove Forest Changes in the Indian Sundarbans from 2000 to 2020. Remote Sens 13, 4957.

Sannigrahi, S., Chakraborti, S., Joshi, P. K., Keesstra, S., Sen, S., Paul, S. K., Kreuter, U., Sutton, P. C., Jha, S., Dang, K. B., 2019. Ecosystem service value assessment of a natural reserve region for strengthening protection and conservation. Journal of Environmental Management 244, 208-227.

Serrano, P. M. L., Rivas, J. J. C., Varela, R. A. D., González, J. G. A., Sánchez, C. A. L., 2016. Evaluation of Radiometric and Atmospheric Correction Algorithms for Aboveground Forest Biomass Estimation Using Landsat 5 TM Data. Remote Sens 8, 369. https://doi:10.3390/rs8050369

Sinha P, Kumar L, Drielsma M, Barrett T., 2014. Time-series effective habitat area (EHA) modeling using cost-benefit raster based technique. Ecol Inform 19:16-25.

Smith, M. J., 2015., A Comparison of DG AComp, FLAASH and QUAC Atmospheric Compensation Algorithms Using WorldView-2 Imagery. Department of Civil Engineering Master's Report University of Colorado.

Stehman, S. V., 1996. Estimating the kappa coefficient and its variance under stratified random sampling. PE & RS. ASPRS, 401-407.

Talukdar, S., Singha, P., Mahato, S., Shahfahad., Pal, S., Liou, Y., Rahman, A., 2020. Land-Use Land-Cover Classification by Machine Learning Classifiers for Satellite Observations-A Review. Remote Sensing 12, 1135

Tucker, C. J., Grant, D. M., Dykstra, J. D., 2004. NASA's global orthorectified landsat data set. Photogrammetric Engineering and Remote Sensing 70, 313-322.

Vaglio Laurin, G., Hawthorne, W., Chiti, T., Di Paola, A., Cazzolla Gatti, R., Marconi, S., Noce, S., Grieco, E., Pirotti, F., Valentini, R., 2016. Does degradation from selective logging and illegal activities differently impact forest resources? A case study in Ghana. iForest - Biogeosciences For. e1–e9.

Zhang, K., Dong, X., Liu, Z., Gao, W., Hu, Z., Wu, G., 2015. Mapping Tidal Flats with Landsat 8 Images and Google Earth Engine: A Case Study of the China's Eastern Coastal Zone circa 2015. Remote Sens 11, 924.